Electronic Supplementary Information

Experimental Section

Materials: Sodium nitrate ($NaNO_3$, 99.0%), sodium nitrite ($NaNO_2$, 99.0%), sodium sulfate (Na_2SO_4), ammonium chloride (NH_4Cl), sodium hydroxide (NaOH), sodium salicylate ($C_7H_5NaO_3$), trisodium citrate dihydrate ($C_6H_5Na_3O_7 \cdot 2H_2O$), p-dimethylaminobenzaldehyde ($C_9H_{11}NO$), sodium nitroferricyanide dihydrate ($C_5FeN_6Na_2O \cdot 2H_2O$), $Na^{15}NO_3$, deuterium oxide (D_2O), 0.8 wt% sulfamic acid solution (H_3NO_3S) and sodium hypochlorite solution (NaClO) were purchased from Aladdin Ltd. (Shanghai, China). Cobalt chloride hexahydrate ($CoCl_2 \cdot 6H_2O$), and ammonium sulfate ($(NH_4)_2SO_4$) were purchased from Chengdu Kelong Chemical Regent Co. Ltd. Sodium hypophosphite (NaH_2PO_2) was bought from Shanghai Macklin Biochemical Co., Ltd. Sulfuric acid (H_2SO_4), hydrogen peroxide (H_2O_2), hydrochloric acid (HCl), hydrazine monohydrate ($N_2H_4 \cdot H_2O$) and ethylalcohol (C_2H_5OH) were bought from Beijing Chemical Corporation. (China). chemical Ltd. in Chengdu. Titanium plate (0.2 mm thick) was purchased from Qingyuan Metal Materials Co., Ltd (Xingtai, China). All reagents used in this work were analytical grade without further purification.

Preparation of Co−P/TP: In brief, $CoCl_2 \cdot 6H_2O$ (1.19 g), $(NH_4)_2SO_4$ (3 g), $C_6H_5Na_3O_7 \cdot 2H_2O$ (3 g) and NaH_2PO_2 (3 g) were dissolved in 50 mL ultrapure water as the electroplating solution. Then, a piece of TP (1 × 1 cm^2) as the working electrode was polarized at −1.0 V (vs. SCE) in the above solution for 30 min, with the use of a carbon rod as the auxiliary electrode and a SCE as the reference electrode to obtain Co−P/TP.

Characterizations: XRD data were acquired by a LabX XRD-6100 X-ray diffractometer with a Cu Kα radiation (40 kV, 30 mA) of wavelength 0.154 nm (SHIMADZU, Japan). SEM measurements were carried out on a GeminiSEM 300 scanning electron microscope (ZEISS, Germany) at an accelerating voltage of 5 kV. XPS measurements were performed on an ESCALABMK II X-ray photoelectron spectrometer using Mg as the exciting source. The absorbance data of

spectrophotometer was measured on UV-Vis spectrophotometer. The ion chromatography data were collected on Metrohm 940 Professional IC Vario. All ^{1}H nuclear magnetic resonance (^{1}H NMR) spectra were collected on Varian VNMRS 600 MHz (the USA) with water suppression.

Electrochemical measurements: All electrochemical measurements were carried on the CHI760E electrochemical workstation (Shanghai, Chenhua) using a standard three-electrode setup. Electrolyte solution was Ar-saturated of 0.2 M Na_2SO_4 with 200 ppm NO_3^-, using Co−P/TP (1 × 1 cm^2) as the working electrode, a carbon rod as the counter electrode and SCE as the reference electrode. We use a H-type electrolytic cell separated by a Nafion 117 Membrane which was protonated by boiling in ultrapure water, H_2O_2 (5%) aqueous solution and 0.5 M H_2SO_4 at 80 °C for another 2 h, respectively. All the potentials reported in our work were converted to reversible hydrogen electrode (RHE) scale via calibration with the following equation: E (RHE) = E (vs. SCE) + 0.0591 × pH + 0.2415 V and the presented current density was normalized to the geometric surface area.

Determination of NH_3 using the indophenol blue method: Concentration of produced NH_3 was determined by spectrophotometry measurement with indophenol blue method (the obtained electrolyte was diluted 100 times).[1] In detail, 4 mL electrolyte was obatined from the cathodic chamber and mixed with 50 μL oxidizing solution containing NaClO (4.5%) and NaOH (0.75 M), 500 μL coloring solution containing $C_7H_5O_3Na$ (0.4 M) and NaOH (0.32 M), and 50 μL catalyst solution $Na_2Fe(CN)_5NO{\cdot}2H_2O$ (1 wt%) for 1 h. The concentration-absorbance curve was calibrated using the standard NH_4Cl solution with NH_3 concentrations of 0.0, 0.05, 0.10, 0.15, 0.20, 0.25 and 0.50 μg mL^{-1} in 0.2 M Na_2SO_4. These solutions were identified via UV-Vis spectroscopy at the wavelength of 660 nm. The concentration-absorbance curves were calibrated using standard NH_3 solution with a serious of concentrations. The fitting curve ($y = 0.62334x + 0.02668$, $R^2 = 0.99983$) shows good linear relation of absorbance value with NH_3 concentration.

Determination of NH_3 using the ^1H NMR spectroscopy: The amount of produced NH_3 was also determined by the ^1H NMR spectroscopy. After chronoamperometry tests in Ar-saturated 0.2 M Na_2SO_4 with 200 ppm NO_3^- at -0.6 V vs. RHE for 2h, the pH of the post-electrolysis electrolyte was adjusted to be 2 with a 0.5 M HCl solution. Then, 0.5 mL of electrolyte and 0.05 mL of deuterium oxide (D_2O) were added into the NMR tube for further NMR (600 MHz) detection. The isotopic labeling experiment was conducted to confirm the origin of ammonium using Ar-saturated 0.2 M Na_2SO_4 with 200 ppm $^{15}NO_3^-$ as the electrolyte in the same operation described above.

Determination of NO_3^-: The amount of NO_3^- was analyzed by spectrophotometry.[2] Firstly, 1.0 mL electrolyte was taken out from the electrolytic cell and diluted to 5 mL to detection range. Then, 0.1 mL 1 M HCl and 0.01 mL 0.8 wt% H_3NO_3S solution were added into the aforementioned solution. After 15 minutes, the absorbance was detected by UV-Vis spectrophotometry at a wavelength of 220 nm and 275 nm. The final absorbance of NO_3^- was calculated based on the following equation: $A=A_{220nm} - 2A_{275nm}$. The calibration curve can be obtained through different concentrations of $NaNO_3$ solutions and the corresponding absorbance. The fitting curve ($y = 0.05841x + 0.0027$, $R^2 = 0.99936$) shows good linear relation of absorbance value with NO_3^- concentration.

Determination of N_2H_4: In this work, we used the method of Watt and Chrisp[3] to estimate whether N_2H_4 produced. The chromogenic reagent was a mixed solution of 5.99 g $C_9H_{11}NO$, 30 mL HCl and 300 mL C_2H_5OH. In detail, 1 mL electrolyte was added into 1 mL prepared color reagent and stirred 15 min in the dark. The absorbance at 455 nm was measured to quantify the N_2H_4 concentration with a standard curve of hydrazine ($y = 0.65546x + 0.0556$, $R^2 = 0.99998$).

Calculations of the conversion rate, FE and NH_3 yield rate:

The conversion rate of NO_3^- is calculated using the following equation:

$$\text{Conversion rate} = \Delta[NO_3^-] / [NO_3^-] \times 100\% \quad (1)$$

FE toward NH_3 via NO_3^- reduction reaction (NO_3^-RR) was calculated by the following equation:

$$FE = (8 \times F \times [NH_3] \times V) / (M_{NH3} \times Q) \times 100\% \quad (2)$$

FE toward NH_3 via NO_2^-RR was calculated by the following equation:

$$FE = (6 \times F \times [NH_3] \times V) / (M_{NH3} \times Q) \times 100\% \quad (3)$$

(Note that the reduction of NO_3^- / NO_2^- to NH_3 consumes eight / six electrons.)

NH_3 yield rate is calculated using the following equation:

$$NH_3 \text{ yield rate} = ([NH_3] \times V) / (M_{NH3} \times t \times A) \quad (4)$$

Where F is the Faradic constant (96485 C mol^{-1}), $[NH_3]$ is the measured NH_3 concentration, $[NO_3^-]$ is the initial concentration of NO_3^-, $\Delta[NO_3^-]$ is the concentration difference of NO_3^- before and after electrolysis, V is the volume of electrolyte in the anode compartment (35 mL), M_{NH3} is the molar mass of NH_3, Q is the total quantity of applied electricity; t is the electrolysis time and A is the loaded area of catalyst (1 × 1 cm^2).

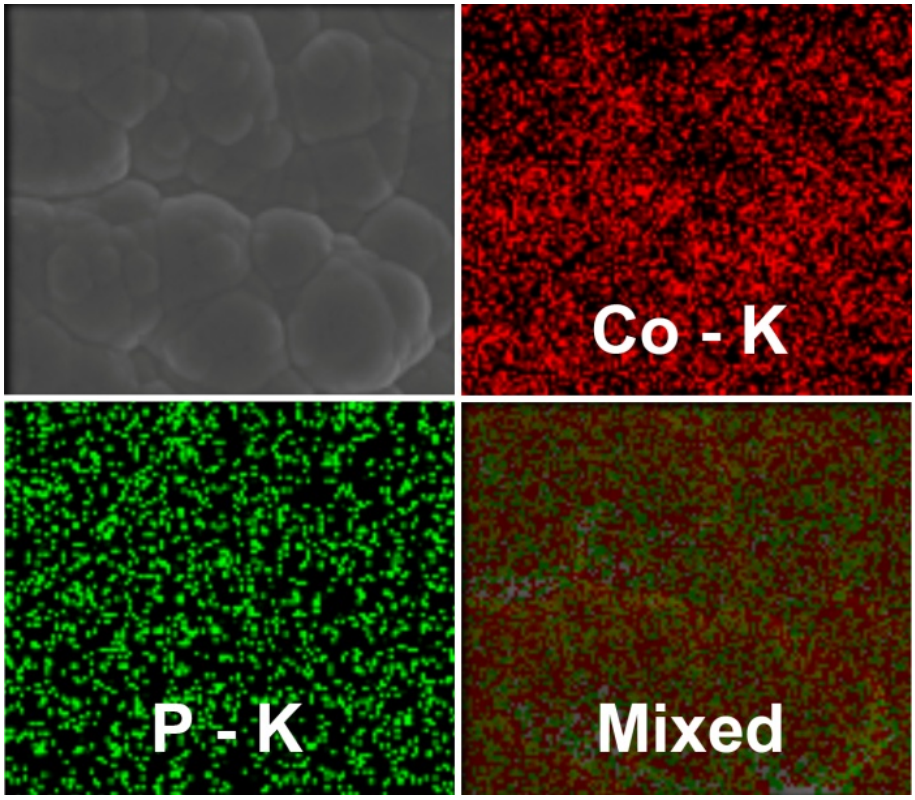

Fig. S1. SEM and EDX elemental mapping images of Co−P/TP.

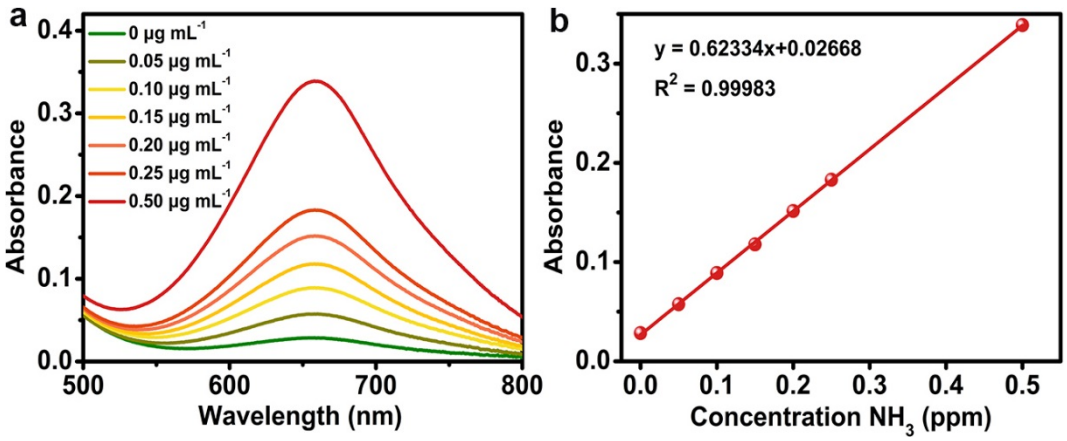

Fig. S2. (a) UV-Vis absorption spectra and corresponding (b) calibration curve used for calculation of NH_3 concentration.

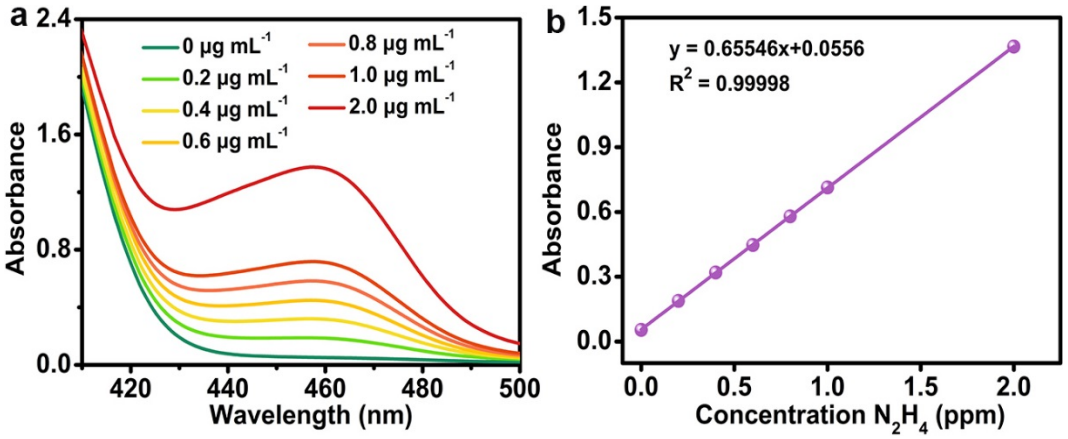

Fig. S3. (a) UV-Vis absorption spectra and corresponding (b) calibration curve used for calculation of N_2H_4 concentration.

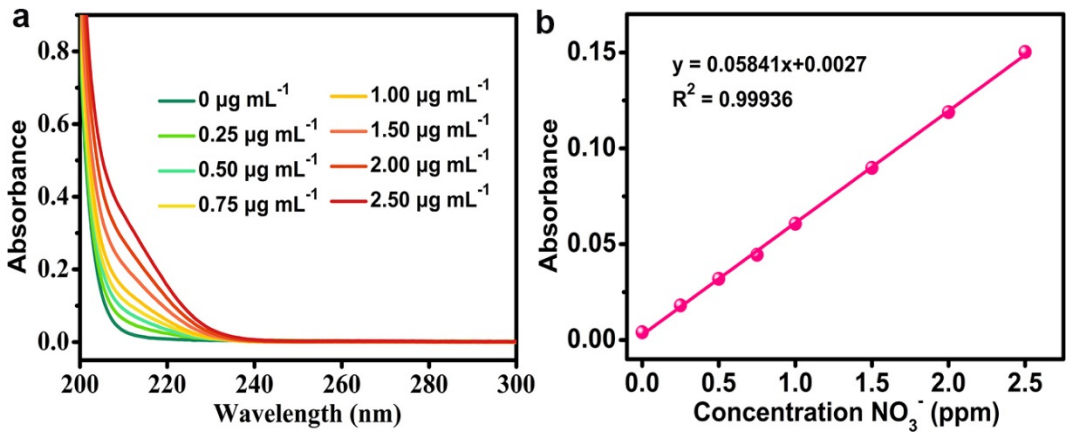

Fig. S4. (a) UV-Vis absorption spectra and corresponding (b) calibration curve used for calculation of NO_3^- concentration.

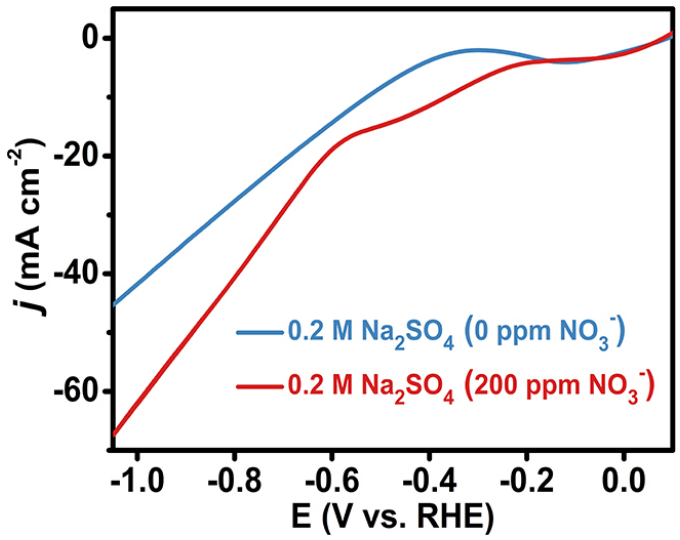

Fig. S5. LSV curves of Co−P/TP tested in 0.2 M Na_2SO_4 with and without 200 ppm NO_3^-.

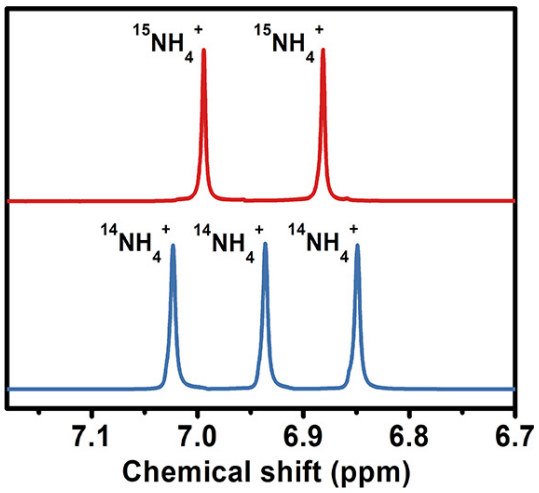

Fig. S6. ^{1}H NMR spectrum for the products using $Na^{14}NO_3$ and $Na^{15}NO_3$ as nitrogen sources.

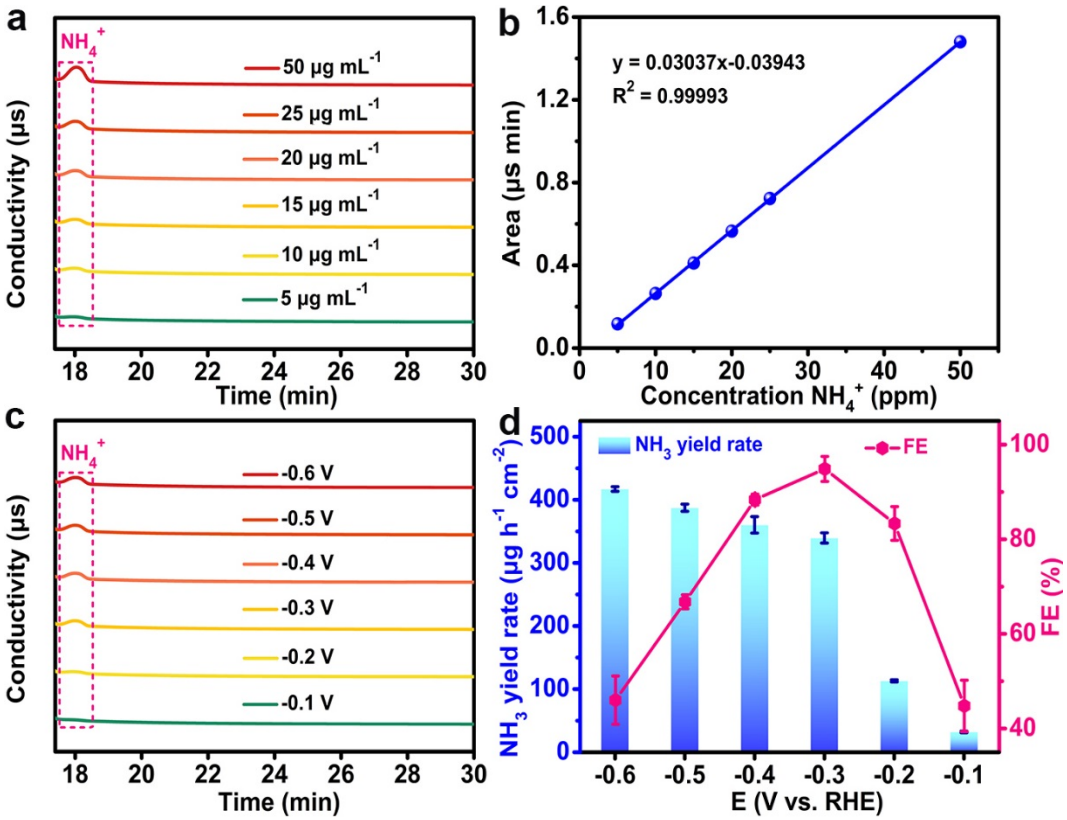

Fig. S7. (a) Ion chromatograms of NH_4^+ with different concentrations in 0.2 M Na_2SO_4 and (b) corresponding standard curve. (c) Ion chromatograms for the electrolytes at a series of potentials after 2 h electrolysis. (d) NH_3 yield rates and FEs of Co−P/TP at corresponding potentials.

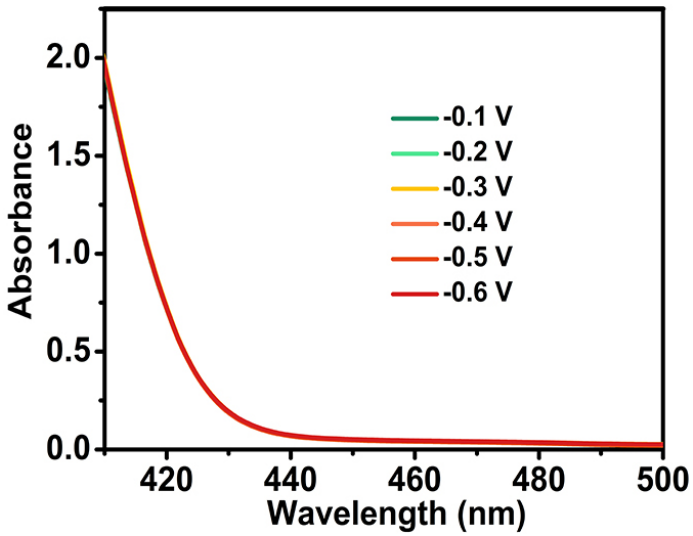

Fig. S8. UV-Vis absorption spectra of the electrolytes estimated by the method of Watt and Chrisp after 2 h electrolysis at each given potential under ambient conditions.

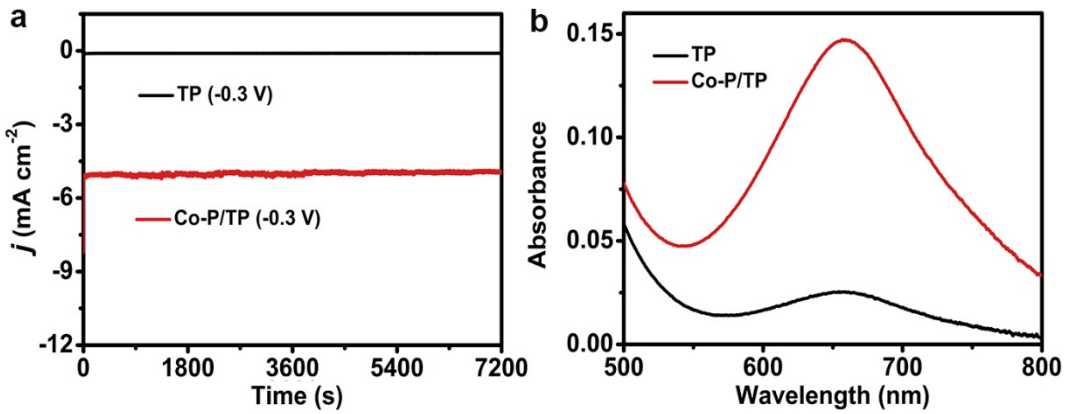

Fig. S9. (a) Time-dependent current density curves of Co−P/TP and bare TP for NO_3^- RR at –0.3 V vs. RHE in 0.2 M Na_2SO_4 with 200 ppm NO_3^-. (b) UV-Vis absorption spectra of the electrolytes stained with indophenol indicator after NO_3^-RR electrolysis.

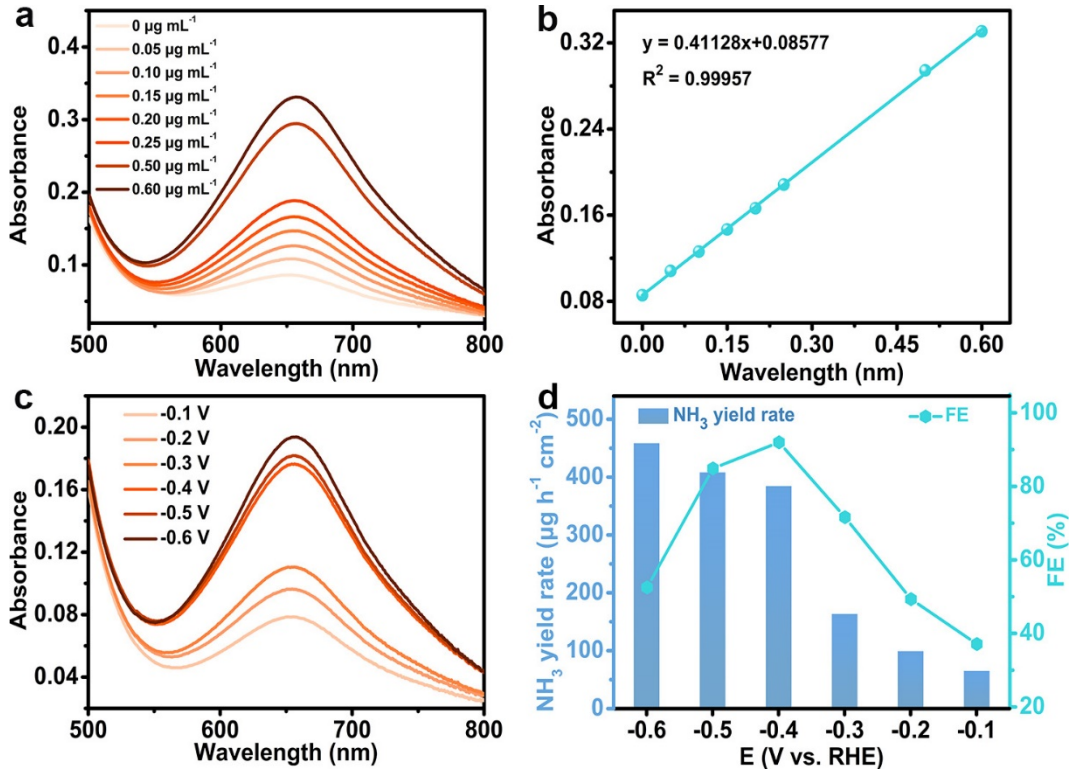

Fig. S10. (a) UV-Vis absorption spectra and corresponding (b) calibration curve used for calculation of NH_3 concentration. Electrochemical tests of Co−P/TP in a two-compartment cell toward NO_3^-RR in 0.2 M PBS with 200 ppm NO_3^- (c) UV-Vis absorption spectra of NH_3. (d) Calculated FEs and NH_3 yield rates of Co–P/TP toward NO_3^-RR at different given potentials.

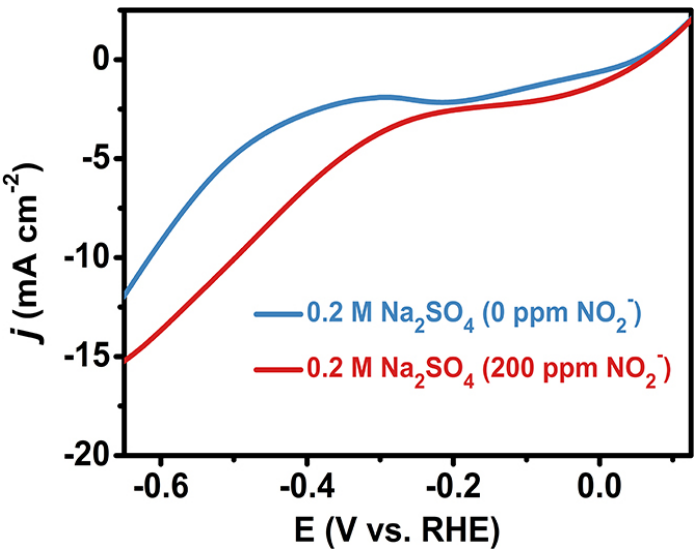

Fig. S11. LSV curves of Co−P/TP tested in 0.2 M Na_2SO_4 with and without 200 ppm NO_2^-.

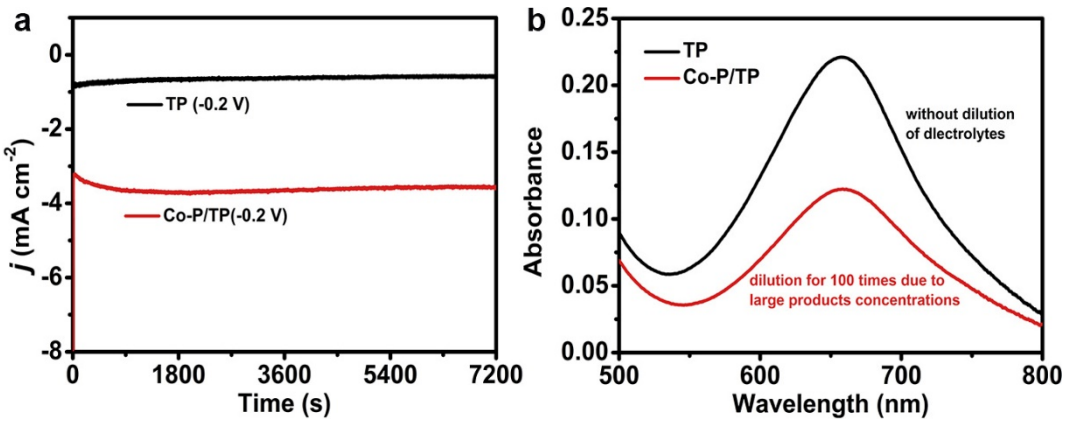

Fig. S12. (a) Time-dependent current density curves of Co−P/TP and bare TP for NO_2^-RR at –0.2 V in 0.2 M Na_2SO_4 with 200 ppm NO_2^-. (b) UV-Vis absorption spectra of the electrolytes stained with indophenol indicator after NO_2^-RR electrolysis.

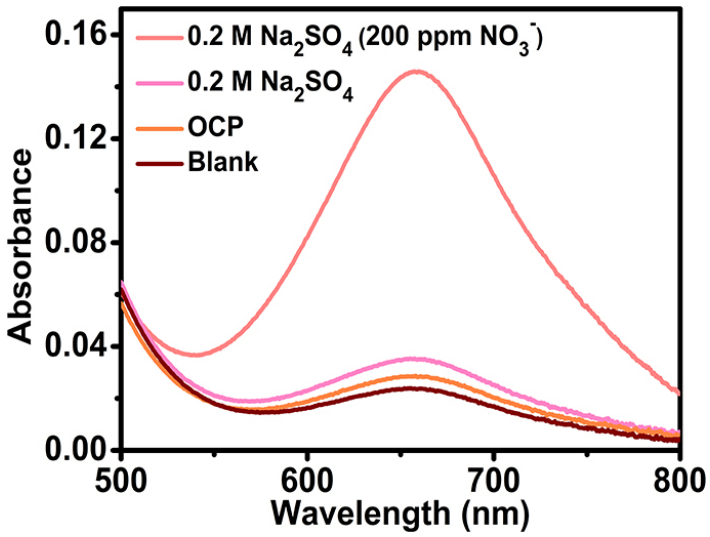

Fig. S13. UV-Vis absorption spectra for different operating conditions.

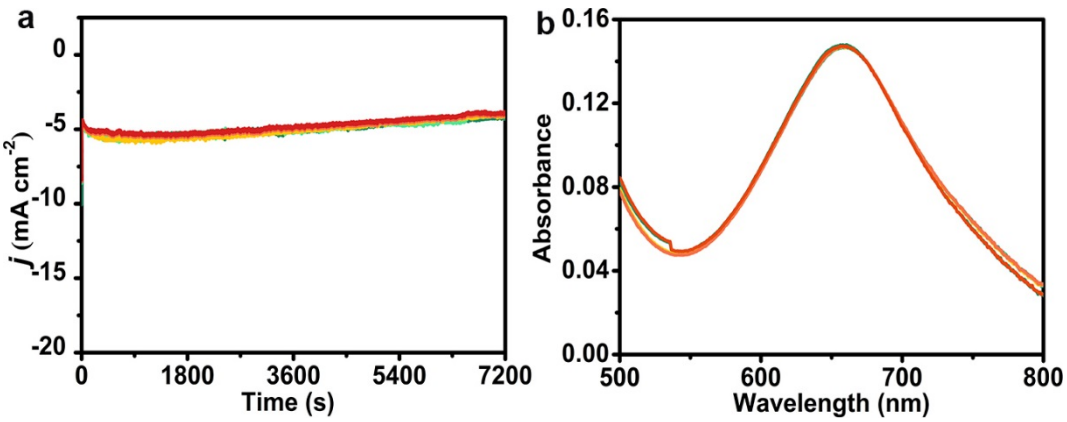

Figure S14. (a) Chronoamperometry curves for Co−P/TP during recycling tests toward NO_3^-RR at –0.3 V in 0.2 M Na_2SO_4 with 200 ppm NO_3^-. (b) UV-Vis absorption spectra for NH_3 and during recycling tests for NO_3^-RR at –0.3 V in 0.2 M Na_2SO_4 with 200 ppm NO_3^-.

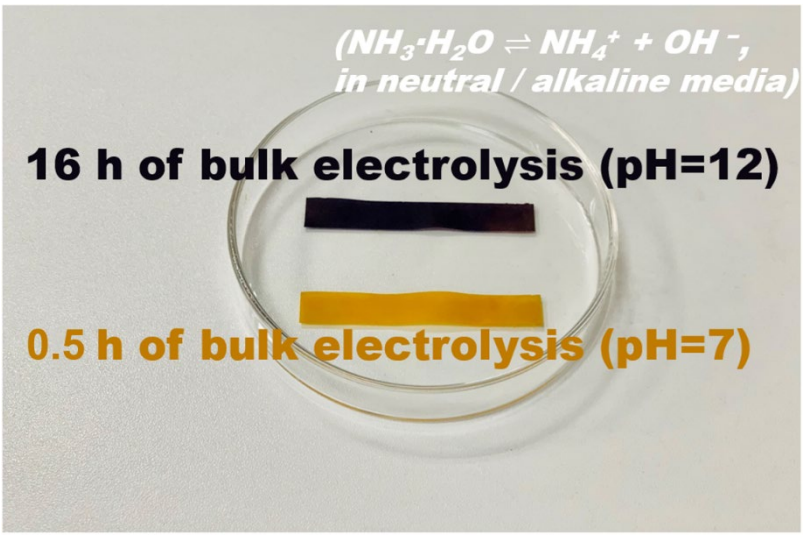

Fig. S15. Photographs of pH test strips with 0.5 h of bulk electrolysis and 16 h of bulk electrolysis.

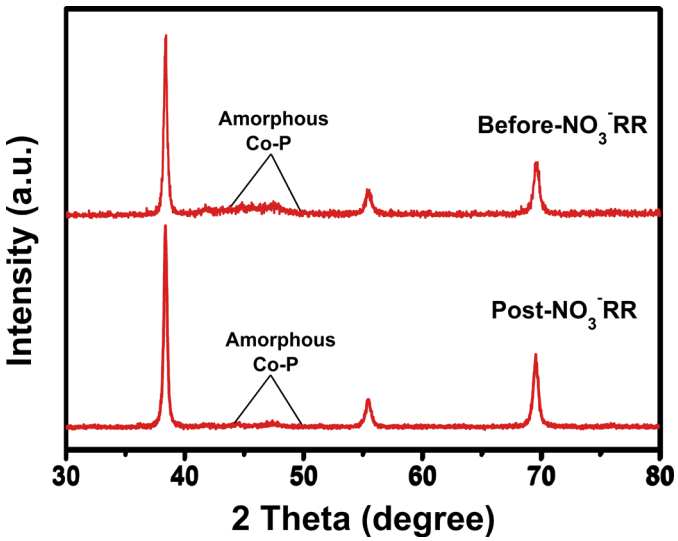

Fig. S16. XRD patterns for Co–P/TP before and after NO_3^-RR.

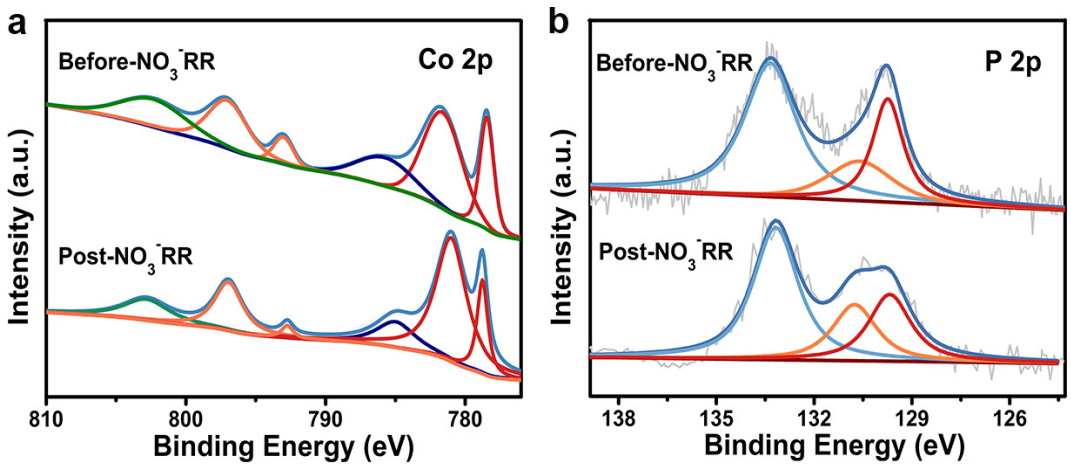

Fig. S17. XPS spectra in the Co 2p and P 2p regions for Co–P/TP before and after NO_3^-RR.

Table S1. Comparison of catalytic performances of Co−P/TP with other reported NO_3^-RR electrocatalysts.

Catalyst	Electrolyte	Performance	Ref.
Co−P/TP	0.2 M Na_2SO_4 (200 ppm NO_3^-)	NH_3 yield rate: 416.0 ± 7.2 μg h^{-1} cm^{-2} (–0.6 V), FE_{NH3}: 93.6 ± 3.3% (–0.3 V), Conversion $rate_{NH3}$: 86.9% (–0.3 V, 10 h)	This work
Cu nanosheets	0.1 M KOH	NH_3 yield rate: 390.1 μg h^{-1} mg^{-1} FE_{NH3}: 99.7%	4
PTCDA/O-Cu	0.1 M PBS (500 ppm NO_3^-)	NH_3 yield rate: 436 ± 85 μg h^{-1} cm^{-2} FE_{NH3}: 85.9%	5
Pd-In/c-Al_2O_3	3.28 mM $NaHCO_3$ with nitrate-reservoir	FE_{NH3}: 71.5%	6
Co_3O_4@NiO HNTs	0.5 M Na_2SO_4 (200 ppm NO_3^-)	NH_3 yield rate: 6.93 mmol h^{-1} g^{-1} FE_{NH3}: 54.97%	7
NiPc complex	0.1 M KOH, in the presence of NO_3^-	FE_{NH3}:85%	8
Cu	1 M NaOH (0.1 M $NaNO_3$)	FE_{NH3}:79%	9
$Cu_{50}Ni_{50}$	1 M KOH (10 mM KNO_3)	FE_{NH3}:84 ± 2%	10
Ti/GC	KOH (~0.1 to 0.6 M NO_3^-)	FE_{NH3}:82%	11
NTEs	NaCl (0.65 mM $NaNO_3$)	FE_{NH3}:5.6%	12

Table S2. Comparison of the catalytic performances of Co−P/TP with other reported NO_2^-RR electrocatalysts under ambient conditions.

Catalyst	Electrolyte	Performance	Ref.
Co−P/TP	0.2 M Na_2SO_4 (200 ppm NO_2^-)	NH_3 yield rate: 661.0 ± 20.1 μg h^{-1} cm^{-2} (–0.6 V), FE_{NH3}: 93.3 ± 3.2% (–0.2 V)	This work
MnO_2 nanoarrays	0.1 M Na_2SO_4 ($NaNO_2$)	NH_3 yield rate: 3.09 × 10^{-11} mol s^{-1} cm^{-2}, FE_{NH3}: 6%	13
Cobalt-tripeptide complex	1.0 M MOPS (1.0 M $NaNO_2$)	NH_3 yield rate: 3.01 × 10^{-10} mol s^{-1} cm^{-2}, FE_{NH3}: 90 ± 3%	14
Poly-NiTRP complex	0.1 M $NaClO_4$ ($NaNO_2$)	NH_3 yield rate: 1.1 mM	15
Cu phthalocyanine complexes	0.1 M KOH ($NaNO_2$)	FE_{NH3}: 78%	16
$[Co(DIM)Br_2]^+$ (Carbon rod working electrode)	0.1 M solution of $NaNO_2$	FE_{NH3}: 88%	17
$Cu_{80}Ni_{20}$	1.0 M NaOH (20 mM $NaNO_2$)	FE_{NH3}: 87.6%	18

References

1 D. Zhu, L. Zhang, R. E. Ruther and R. J. Hamers, *Nat. Mater.,* 2013, **12**, 836–841.

2 Y. Wang, W. Zhou, R. Jia, Y. Yu and B. Zhang, *Angew. Chem. Int. Ed.,* 2020, **132**, 5388–5392.

3 G. W. Watt and J. D. Chrisp, *Anal. Chem.,* 1952, **24**, 2006–2008.

4 X. Fu, X. Zhao, X. Hu, K. He, Y. Yu, T. Li, Q. Tu, X. Qian, Q. Yue, M. Wasielewski and Y. Kang, *Appl. Mater. Today,* 2020, **19**, 100620.

5 G. Chen, Y. Yuan, H. Jiang, S. Ren, L. Ding, L. Ma, T. Wu, J. Lu and H Wang, *Nat. Energy,* 2020, **5**, 605–613.

6 B. P. Chaplin, J. R. Shapley and C. J. Werth, *Catal. Lett.,* 2009, **130**, 56–62.

7 Y. Wang, C. Liu, B. Zhang and Y. Yu, *Sci. China Mater.,* 2020, **63**, 2530–2538.

8 N. Chebotareva and T. Nyokong, *J. Appl. Electrochem.,* 1997, **27**, 975–981.

9 D. Reyter, G. Chamoulaud, D. Bélanger and L. Roué, *J. Electroanal. Chem.,* 2006, **596**, 13–24.

10 Y. Wang, A. Xu, Z. Wang, L. Huang, J. Li, F. Li, J. Wicks, M. Luo, D. H. Nam, C. Tan, Y. Ding, J. Wu, Y. Lum, C. T. Dinh, D. Sinton, G. Zheng and E. H. Sargent, *J. Am. Chem. Soc.,* 2020, **142**, 5702–5708.

11 J. M. McEnaney, S. J. Blair, A. C. Nielander, J. A. Schwalbe, D. M. Koshy, M. Cargnello and T. F. Jaramillo, *ACS Sustainable Chem. Eng.,* 2020, **8**, 2672−2681.

12 X. Ma, M. Li, C. Feng, W. Hu, L. Wang and X. Liu, *J. Electroanal. Chem.,* 2016, **782**, 270−277.

13 R. Wang, Z. Wang, X. Xiang, R. Zhang, X. Shi and X. Sun, *Chem. Commun.,* 2018, **54**, 10340–10342.

14 Y. Guo, J. R. Stroka, B. Kandemir, C. E. Dickerson and K. L. Bren, *J. Am. Chem. Soc.,* 2018, **140**, 16888–16892.

15 P. Dreyse, M. Isaacs, K. Calfumán, C. Cáceres, A. Aliaga, M. J. Aguirre and

D. Villagra, *Electrochim. Acta,* 2011, **56**, 5230–5237.

16 N. Chebotareva and T. Nyokong, *J. Appl. Electrochem.,* 1997, **27**, 975–981.

17 S. Xu, H. Y. Kwon, D. C. Ashley, C. H. Chen, E. Jakubikova and J. M. Smith, *Inorg. Chem.,* 2019, **58**, 9443–9451.

18 L. Mattarozzi, S. Cattarin, N. Comisso, P. Guerriero, M. Musiani, L. Vázquez-Gómez and E. Verlato, *Electrochim. Acta,* 2013, **89**, 488–496.